

Article

Benchmark Dataset for Offshore Platform Motion Prediction and Its Applications

Wenyin Pan ^{1,2} , Xiaoxian Guo ^{1,2,*} and Xin Li ^{1,2}

¹ SJTU Yazhou Bay Institute of Deep-Sea Technology, Sanya 572000, China; victorppp98@gmail.com (W.P.); lixin@sjtu.edu.cn (X.L.)

² State Key Laboratory of Ocean Engineering, Shanghai Jiao Tong University, Shanghai 200240, China

* Correspondence: xiaoxguo@sjtu.edu.cn

Abstract: The accurate prediction of offshore platform and ship motion is crucial for motion compensation devices and for helping the crew make informed decisions. Traditional time series and physical models are being replaced by machine learning models due to their simplicity and lower training cost. However, insufficient data has hindered model training, making evaluating and comparing different models difficult. This paper introduces a comprehensive motion dataset containing data of more than 400 pieces from tens of offshore platform tests conducted at the State Key Laboratory of Ocean Engineering, Shanghai Jiao Tong University. The dataset is divided into subsets tailored for four application scenarios, including specific types of offshore platforms, wave conditions, noise addition data, and transfer learning. A Convolutional Attention-based LSTM model that combines convolution and self-attention mechanisms is proposed to validate the dataset and improve the accuracy of motion prediction. The proposed model is compared with classical models using our introduced dataset, achieving 5–10% improvement and confirming the dataset's high reliability and applicability, as well as the effectiveness of the Conv-Att-LSTM model. This development sets a new standard for motion prediction and furthers the application of machine learning in ocean engineering.

Keywords: motion dataset; real-time motion prediction; machine learning; LSTM; self-attention



Citation: Pan, W.; Guo, X.; Li, X. Benchmark Dataset for Offshore Platform Motion Prediction and Its Applications. *J. Mar. Sci. Eng.* **2024**, *12*, 1852. <https://doi.org/10.3390/jmse12101852>

Academic Editor: Vincenzo Crupi

Received: 19 August 2024

Revised: 10 October 2024

Accepted: 15 October 2024

Published: 17 October 2024



Copyright: © 2024 by the authors. Licensee MDPI, Basel, Switzerland. This article is an open access article distributed under the terms and conditions of the Creative Commons Attribution (CC BY) license (<https://creativecommons.org/licenses/by/4.0/>).

1. Introduction

Marine offshore platform and ship motions present significant challenges to sensitive offshore operations, such as aircraft landing on carriers, rocket launches from vessels, heavy lifting by floating cranes, and dynamic positioning control [1]. Variations in environmental factors, such as waves, wind, and ocean currents, can result in significant motion changes in offshore platforms and ships. Generally, six degrees of freedom (6 DoFs) motions can be modeled as a linear mass-damping spring system, and its equations of motion can be governed by coefficients of mass-damping spring and the external forces applied to it with Newton's second law. Real-time motion prediction, unlike long-term or short-term motion forecasting [2], for offshore platforms or vessels focuses on predicting motions within the next several tens of seconds (equivalent to one or two wave periods). Accurate predictions can enhance motion compensation systems and offer valuable early warning information critical for operational safety and efficiency [3].

Numerous studies have been conducted to develop motion prediction methods for marine offshore platforms and ships. In an early study, Kaplan [4] proposed a convolution method for ship motion prediction, using the Wiener filter to forecast the motion response of an aircraft carrier. In pioneering studies [5,6], state-space models based on Kalman filtering techniques were employed, thus necessitating comprehensive information regarding wave kinetics and ship dynamics. Owing to the frequency dependencies of added mass, damping, and wave excitation forces, accurately estimating the peak frequency of the wave spectrum is critical. Yumori [7] introduced an auto-regressive (AR) moving average model to predict

ship behavior a few seconds in advance. The AR models are based solely on time series analyses. Duan et al. [8–10] and Jiang et al. [11] investigated the effects of ship hull scale on real-time motion prediction using an AR model. Although different methods are applied in motion prediction for ships and offshore platforms, some disadvantages impede their further application in real-time prediction, e.g., laborious calculations and parameters requiring pre-acknowledgment.

The neural network (NN) approach originated in computer science and relies on the difference between calculated and actual values, iteratively updating model parameters through gradient descent to improve predictions. Due to their ease of modeling, superior performance, and high accuracy, NNs have increasingly surpassed conventional methods for offshore platform and ship motion prediction. Notably, they were first introduced by Lainiotis et al. [12]. In a subsequent study, Khan et al. [13,14] predicted roll motion for up to 7 s using linear NN layers, and Yin et al. [15] combined a discrete wavelet transform with radial basis function networks to enhance accuracy. A recurrent neural network (RNN) is a specific network that considers the inherent order of data. Therefore, RNNs are suitable for applications such as natural language processing and analysis of time-series data and have shown promising results in offshore platform and ship motion prediction [16].

Recently, new motion prediction models have been combined with RNNs and their variants, such as long short-term memory (LSTM) and gated recurrent units. Liu et al. [17,18] predicted the roll motion of a container ship using an LSTM model and optimized the input vector space of the model using techniques based on impulse response and autocorrelation functions. Guo et al. [19] proposed an LSTM model to predict the heave and surge motions of a floating semi-submersible 20–50 s ahead with high accuracy. In addition, they showed that the trained model can operate effectively with noise levels up to a variance of 0.8. The model was further extended via noise incorporation to quantify its uncertainty in predicting time series [20]. Similarly, Sun et al. [21] combined Gaussian process regression (GPR) with LSTM networks to predict ship attitudes (roll and pitch angles). Additionally, Zhang et al. [22] proposed a multiscale attention-based LSTM method, where the motion signal was first decomposed via wavelet transform, and the weights at each scale were obtained via an attention mechanism. Li et al. [23] compared prediction results for 0, 6, and 12 s lead times. Wei et al. [24] and Fu et al. [25] used a bidirectional LSTM NN for ship motion prediction, incorporating empirical wavelet transform and channel attention, respectively. Taskar et al. [26] performed motion prediction based on different wave conditions and discussed the relationship between the length of the input window and the output window. Similarly, Xun et al. [27] proposed a self-attention LSTM (SALSTM) model and verified its effectiveness under three representative working conditions. Recently, several scholars have applied neural networks to various fields of marine engineering. Chen et al. [28] accurately predicted heave, pitch, and roll motions within an 8 s range using an LSTM model, achieving an error of less than 15%, thereby enhancing the safety and efficiency of shipborne helicopter landings. Burak et al. [29] employed an artificial neural network (ANN) to predict the residual resistance coefficient of a trimaran model, effectively replacing traditional model tests and numerical simulations. Ayhan et al. [30] used both an ANN and the Adaptive Neuro-Fuzzy Inference System (ANFIS) to estimate hawser tensions and displacements in a spread mooring system (SMS), successfully solving the optimization design challenges of the SMS. Meanwhile, Ibrahim et al. [31] predicted 14 parameters, such as maximum speed, ship type, and deadweight tonnage (DWT), across different ship types, achieving more accurate results. They also optimized the ANN parameters to further enhance performance. Figure 1 shows an overview of the research development of motion prediction using different methods.

Although many methods demonstrate high prediction accuracy on their respective datasets, comparing these models and methods is not recommended owing to the different datasets used. The scales of the data and the research objects differed significantly between these two studies. Table 1 shows the differences among related studies.

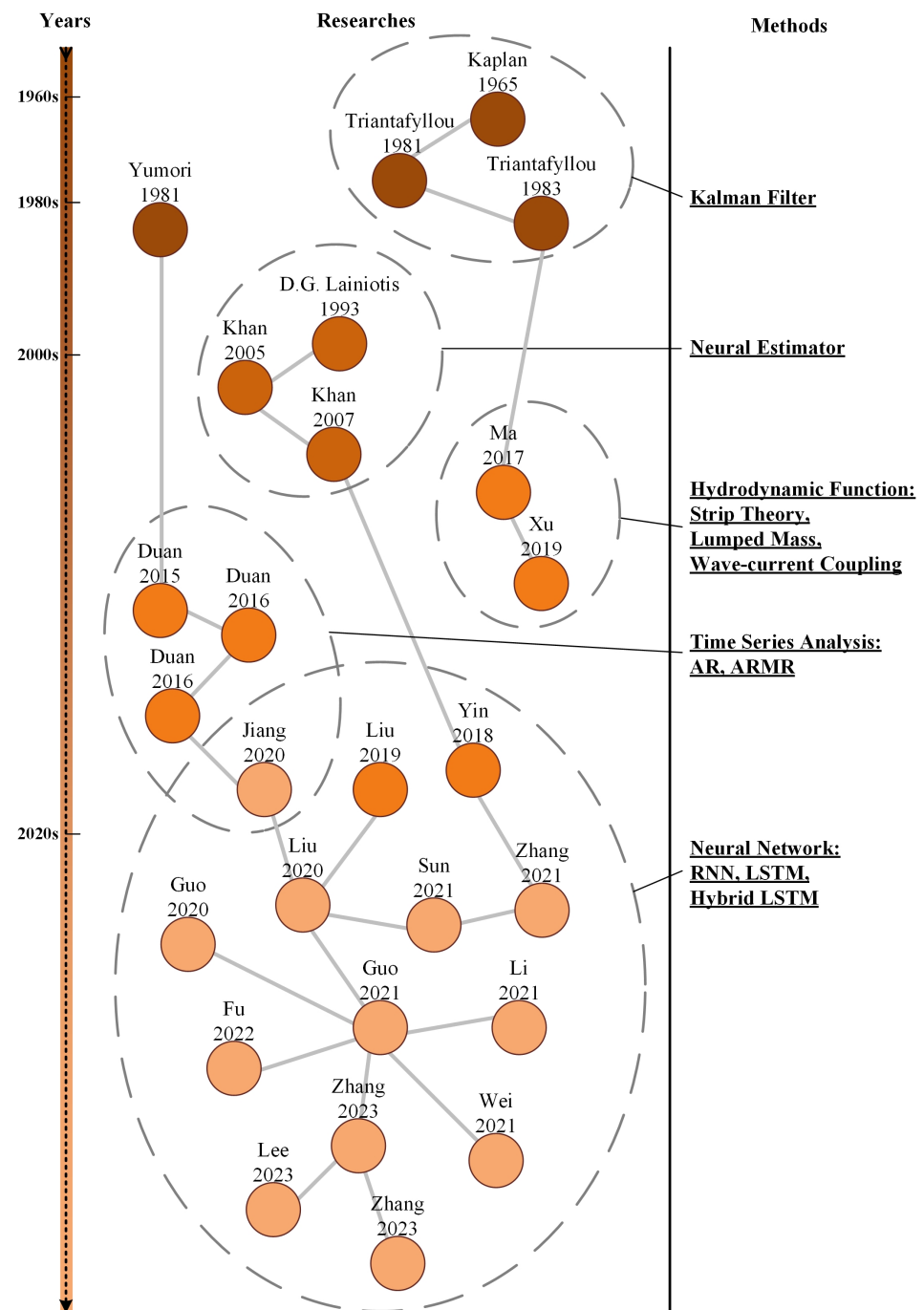


Figure 1. An overview of motion prediction research history [4–15,17–25,32–36].

Quality datasets are crucial for the practical training of NN models. In computer vision, comprehensive datasets, such as ImageNet [37], which contains approximately 15 million images across 22,000 categories, are instrumental. Datasets such as Kinetic [38], UCF [39], and HMDB [40] are crucial in video comprehension and classification. Additionally, well-established datasets such as MNIST [41] for handwritten digit recognition, CelebA [42] for face recognition, and SEED [43] for EEG signal classification are widely used. However, owing to issues such as the confidentiality of motion data, developing a unified and comprehensive dataset remains challenging in ship and ocean engineering. Therefore, a standardized dataset must be established as a benchmark for the training and evaluation of various prediction models. This paper introduces a comprehensive motion dataset from model tests of tens of offshore platforms at the State Key Laboratory of Ocean Engineering

(SKLOE) of Shanghai Jiao Tong University, which has proven effective and robust in different situations. The motion dataset contains data from tens of offshore platforms under various wave conditions from 1-year to 1000-year waves and the data have been cleaned and normalized to ensure the practicality of the dataset. In addition, the dataset has been used in many applications in different scenarios with high reliability.

Table 1. Different datasets and models used in related studies.

Model	Paper	Data Source	Datasets Scale	Prediction Motions
LSTM	[19]	Semi-submersible model (Reduction ratio = 1:60)	8 wave cases	Surge, Heave
LSTM	[20]	Semi-submersible model (Reduction ratio = 1:60)	8 wave cases	Heave
LSTM-GPR	[21]	A large military ship	1000 steps selected from 250 s	Roll, Pitch
MSA-LSTM	[22]	A certain ship	Not mentioned	6 DoFs
LSTM	[23]	Semi-submersible model (Reduction ratio = 1:56)	40 wave cases	Surge, Heave, Pitch
Hybrid BiLSTM	[24]	A scientific research ship (SHIYAN-1)	3 sets of roll series data from 1200 s	Roll
Bi-ConvLSTM-CA	[25]	A certain ship	10,000 s	Pitch

The remainder of this paper is organized as follows: Section 2 introduces and describes the proposed motion dataset, in particular the data sources, platforms, and wave conditions, as well as the methods for data processing. Section 3 presents a Conv-Att-LSTM model for motion prediction and different case studies to assess the reliability of the dataset and shows a comparison among different models trained on the dataset. The experimental results demonstrate that the model achieves superior accuracy in different cases and that the dataset could effectively evaluate the performance of various models. Finally, Section 4 presents detailed information regarding the motion dataset, including its advantages and effectiveness under different scenarios.

2. Motion Dataset

2.1. Data Description

The proposed motion dataset currently contains approximately 200 sets of experimental model test data for more than ten offshore platforms from the SKLOE of Shanghai Jiao Tong University. Each experimental dataset includes the platform's 6 DoF motion and wave time-series data.

Based on experimental wave conditions, the motion time-series data of different platforms were classified and selected for various cases, including 1-year to 1000-year wave conditions. The dataset contains 13 platforms, each categorized into training, validation, and test sets. Figure 2A,B show the relationship between the data over different platforms and wave conditions; Figure 2A shows that the dataset includes a wide range of offshore platforms, and the characteristic length denotes pontoon intervals for semi-submersible platforms or pontoon diameters for FWPSO (floating workover production storage and offloading system); Figure 2B shows 1-year to 1000-year wave conditions in the dataset.

Figure 2C illustrates the cross-correlation between various offshore platform and ship motions and wave patterns. Red indicates a positive correlation, blue signifies a negative correlation, and white indicates the absence of a relationship. Clearly, the wave shows the highest correlation with the heaving motion. Hence, the heave motion is primarily utilized for subsequent predictions.

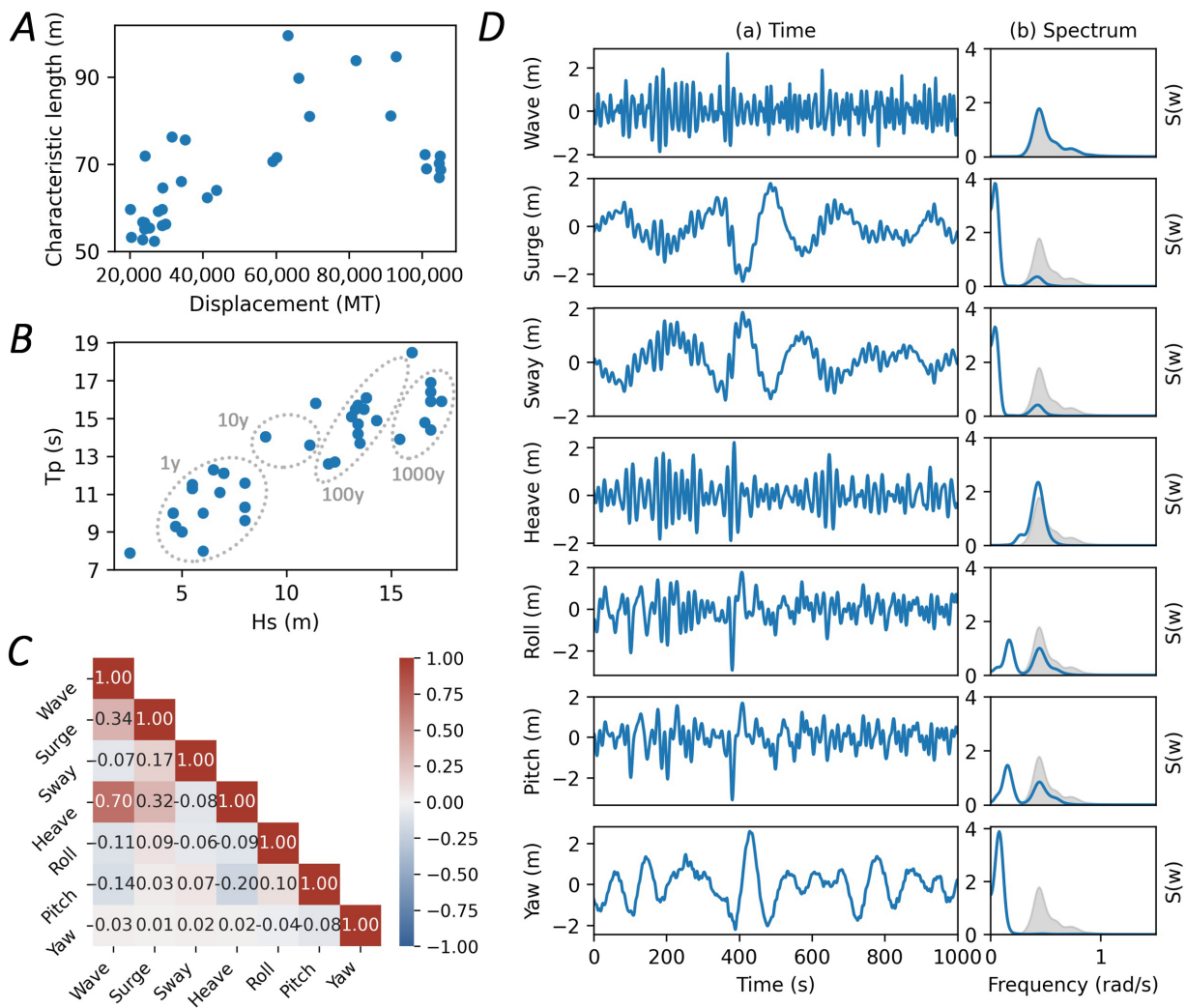


Figure 2. Data description in dataset (A) The dataset includes a wide range of offshore platforms. (B) The dataset includes 1-year to 1000-year wave conditions. Tp stands for average peak period and Hs stands for wave height. (C) Cross-correlation between different channels in the dataset. (D) The time and spectrum domain of wave and motion data

Among the 6 DoF motions, the inherent period of the heave motion is aligned with the general wave frequency range. The heave motion was predominantly affected by wave excitation and characterized by a wave-induced, wave-frequency motion response without low-frequency motion components. Consequently, focusing on the heave motion for motion prediction, particularly when combined with wave time-history information, significantly enhances motion prediction accuracy. This approach is practical for evaluating the performance of the prediction models. Figure 2D provides a spectral analysis of both the motion and wave time-series data, where (a) shows the motions and waves in the time domain and (b) presents the data in the spectrum domain. The gray region in these graphs represents the wave spectrum. Furthermore, this analysis reaffirms that the heave motion is predominantly wave-dominated, thus underscoring its relevance in motion prediction studies.

The proposed dataset extends beyond the cleansing of experimental data. It includes various subsets customized to different usage scenarios, including motion datasets specific to each platform, datasets categorized by wave conditions, datasets with added Gaussian noise, and datasets designed for transfer learning. Each subset was intended to address particular aspects of motion prediction and model training, thus offering a comprehensive

resource for diverse research and applications. The specifics of these datasets are detailed in the following subsection.

2.2. Data Processing

The data were initially recorded in a specific format. The first step in data processing involved cleaning the raw data, which included normalization, phase alignment, and outlier rejection, to ensure data validity. The data-acquisition frequency differed across the trials due to the varying test conditions and experimental environments. All test data were resampled to a consistent frequency of 10 Hz via linear interpolation to standardize the prediction timescale for subsequent analysis. Furthermore, considering the variation in the total sampling duration between experiments, the data were artificially sliced to manage the time-scale length effectively. This approach allows for more controlled management of the total training data volume based on the number of data files used; however, one can continue using the original complete data.

Additionally, the initial and final phases of the experiments, which typically feature prolonged periods of irrelevant data, were removed during the slicing process. This ensures a uniform and relevant dataset for robust analysis and model training. Table 2 shows the data size in the dataset for each platform, including the total number of segments in the dataset and the number of segments for different wave conditions.

Table 2. Statistics of segments on each platform.

Platform	Wave				Total
	1y	10y	100y	1000y	
1	9	18	0	0	27
2	0	7	30	30	67
3	18	0	21	0	39
4	0	0	36	0	36
5	9	9	18	0	36
6	6	6	0	0	12
7	8	0	4	0	12
8	6	0	6	0	12
9	6	0	6	0	12
10	9	0	3	0	12
11	24	0	54	0	78
13	0	0	65	64	129
14	9	0	3	0	12
Total	104	40	246	94	484

After initial processing, all data were stored in pickle files to ensure efficient management. To enhance the utility of the dataset, it was further organized into several subsets, each serving a specific purpose. First, data from identical platforms were clustered into individual datasets. This allows users to train and test their prediction models on different datasets, thereby allowing them to assess the generalization capabilities of the models across various platforms. Second, data under the same wave conditions, ranging from 1-year to 1000-year events, were collated. This subset enables users to evaluate the model performance under different wave intensities, e.g., the model might excel using 10-year data but falter using 1000-year data. Additionally, various levels of Gaussian noise were introduced into the original data via the approach described in [20]; subsequently, the robustness of the prediction models against noise interference was tested. Finally, a comprehensive pretraining dataset was constructed, encompassing data from diverse platforms and under various wave conditions. Users can initially train their models on this mixed dataset and fine-tune them on specific data subsets. This process allows one to determine whether pretraining enhances model performance compared with direct training on the target data. All these steps and the structure of the dataset are depicted in Figure 3, which provides a visual guide for the organization of the dataset and its potential applications.

An open-source dataset demo (Github Link <https://github.com/v1ctorpan/SKLOE-dataset> accessed on 18 August 2024) that contains several data series is available, and users can apply the data to their model training.

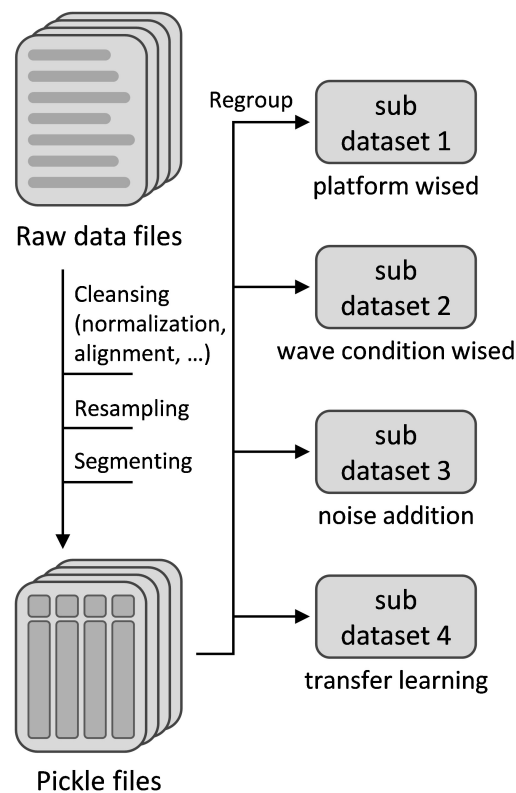


Figure 3. Data processing progress.

3. Case Study

This section presents various case studies conducted using the proposed dataset. In these case studies, the model training and the performance evaluation of the dataset across different scenarios are performed.

- (1) Training on different platforms: This involves assessing the model's adaptability and effectiveness when trained on data from various platforms, thus demonstrating the model's performance across diverse platforms.
- (2) Training under various wave conditions: The models were trained using data representative of wave conditions, as illustrated in Table 2, i.e., from mild to extreme conditions. This evaluates the management and prediction capability of the model under varying environmental factors.
- (3) Training with additional noise conditions: The models were trained on data with added noise levels. This approach evaluates the robustness of the model against disturbances and uncertainties, which are typical in real-world scenarios.
- (4) Performance comparison with and without pretraining: This assesses the effect of pretraining on model performance. The model was trained directly on specific datasets and preliminarily on a broader, mixed dataset. This comparison allows one to determine the effectiveness of pretraining in enhancing the model accuracy and generalizability.

These cases collectively aim to rigorously test the proposed dataset's efficacy in improving the training and performance of predictive models under various maritime conditions. Before discussing the case studies, this paper introduces the predictive model used for dataset testing, as depicted in Figure 4, known as the Conv-Att-LSTM model. This model comprises a sophisticated series of layers, including convolutional layers, which filter data

and eliminate phase, self-attention layers, which further correct the discrepancy between the model’s output and the desired value, recurrent layers, which process time series information, and linear layers for final fitting. Table 3 lists the model’s hyperparameters. The subsequent case studies focus on the model’s performance and validating the dataset’s robustness and applicability in motion prediction. These studies aim to demonstrate that the dataset effectively supports and enhances the model’s predictive capabilities, thereby proving its value and utility in the field.

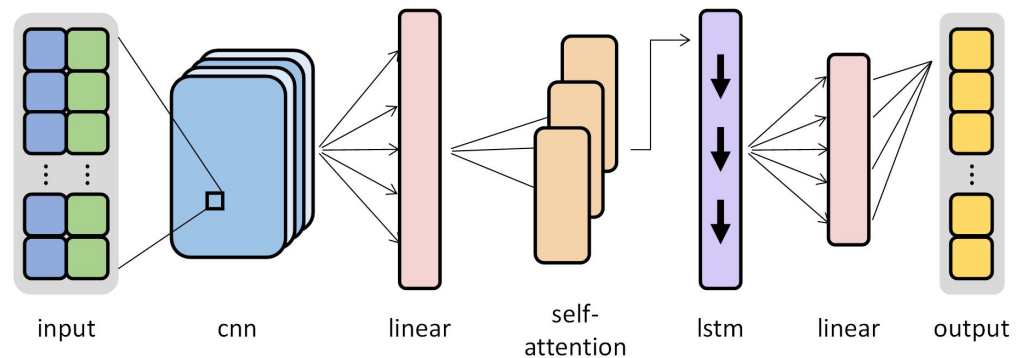


Figure 4. Illustration of Conv-Att-LSTM model.

Table 3. Hyperparameters for Conv-Att-LSTM model.

No.	Layer	Input Dim	Output Dim
1	inputs	-	(-1, 180, 2)
2	cnn	(-1, 180, 2)	(-1, 180, 512)
3	linear—Q, K, V	(-1, 180, 512)	(-1, 180, 512)
4	self-attention	(-1, 180, 512)	(-1, 180, 512)
5	lstm—1~6	(-1, 180, 512)	(-1, 180, 512)
6	linear—1	(-1, 180, 512)	(-1, 180, 256)
7	linear—2~6	(-1, 180, 256)	(-1, 180, 256)
8	outputs	(-1, 180 × 256)	(-1, 60)

3.1. Training on Platform-Based Datasets

The dataset contains data from various platforms, providing users access to training data across different platforms. The experimental conditions, which include environmental and wave conditions, can vary significantly across different experiments. Such variations can manifest in different simulated seawater depths and wave patterns, such as the height and period. Data normalization, segmentation, and other process steps can be performed to ensure accuracy and reliability. Notably, models trained on data from different platforms may yield varying outputs. This is attributable to differences in the structural design of the models.

Therefore, a subset was introduced to show the training on data from these different platforms, which included data from platforms 2, 3, 4, 5, 11, and 13, all of which were under the 100-year wave condition. Data were randomly segregated within each platform into training, validation, and testing sets. Table 2 provides a comprehensive overview of the data from each platform.

Figure 5A shows the model’s results trained on data from the different platforms mentioned earlier. The top chart illustrates the accuracy achieved by training on data from various platforms, which predominantly ranged between 0.7 and 0.9. Platforms 3 and 13 exhibited higher accuracies compared with the other platforms. This shows that the performance of the same model can vary when trained on different datasets. Platforms with higher accuracy can serve as users’ references. The bottom chart shows the loss values across various platforms, with Platform 3 performing commendably in reduced loss.

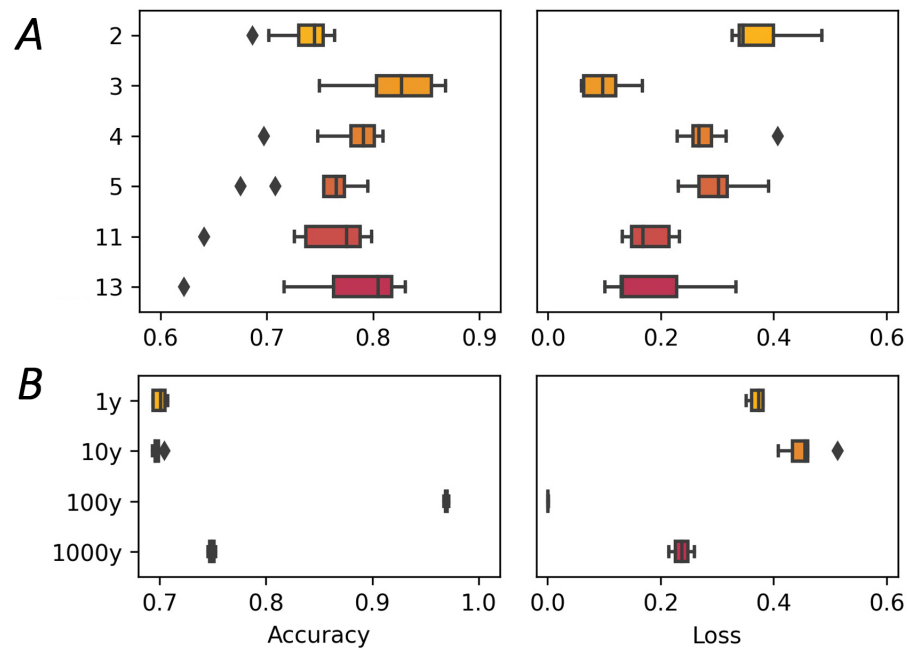


Figure 5. Box plots showing training results on (A) platform-based and (B) wave condition-based subsets. The left and right figures show accuracy and loss variation, respectively.

3.2. Training on Wave-based Datasets

Similarly, a regrouped dataset based on various wave conditions was introduced to provide datasets under different wave conditions. As shown in Table 2, each wave condition contained motion data from several platforms.

Figure 5B illustrates the results of the model trained on data from the various wave conditions. In general, because each wave condition contained data from several different platforms, the accuracy and performance loss during training were not favorable. However, as shown in Section 3.4, by utilizing the abundance of such datasets for pretraining and then fine-tuning specific data, we can significantly reduce the training cost by reducing the training time. Moreover, this approach generalizes the model to some extent, thus resulting in improved accuracy.

3.3. Training on Noise Addition Datasets

In this subsection, we describe how we used the data in the dataset and incorporated further additions and modifications. For the model test data in the datasets, the training data can be increased by adding noise to the data to train the model more effectively. Guo et al. [20] demonstrated that adding an appropriate amount of noise to training data improved the robustness of a model, thus allowing it to adapt to a broader range of noisy input data and provide more accurate motion predictions. Figure 6A shows a comparison before and after noise was added to the dataset. We set two noise specifications to compare whether different noise levels and no-noise data improved or degraded the forecast accuracy during training. Table 4 outlines the specific noise specifications. This methodology is crucial for fine-tuning the model to achieve optimal performance in real-world, noise-affected scenarios.

Table 4. Noise level.

Noise Level	Noise Type	Motion		Wave	
		Mean	Var	Mean	Var
lv. 1	Gauss	0	1	0	1/5
lv. 2	Gauss	0	1	0	1/2

The deep learning prediction models were trained on noise-free data, level 1 noise data, and level 2 noise data, and then finally tested on noise-free data. The variations in the accuracy and loss are shown in Figure 6B, and the final motion prediction obtained is shown in Figure 6C. The figure only shows the motion 40 time steps ahead of the prediction, and the actual model input comprises 180 time steps.

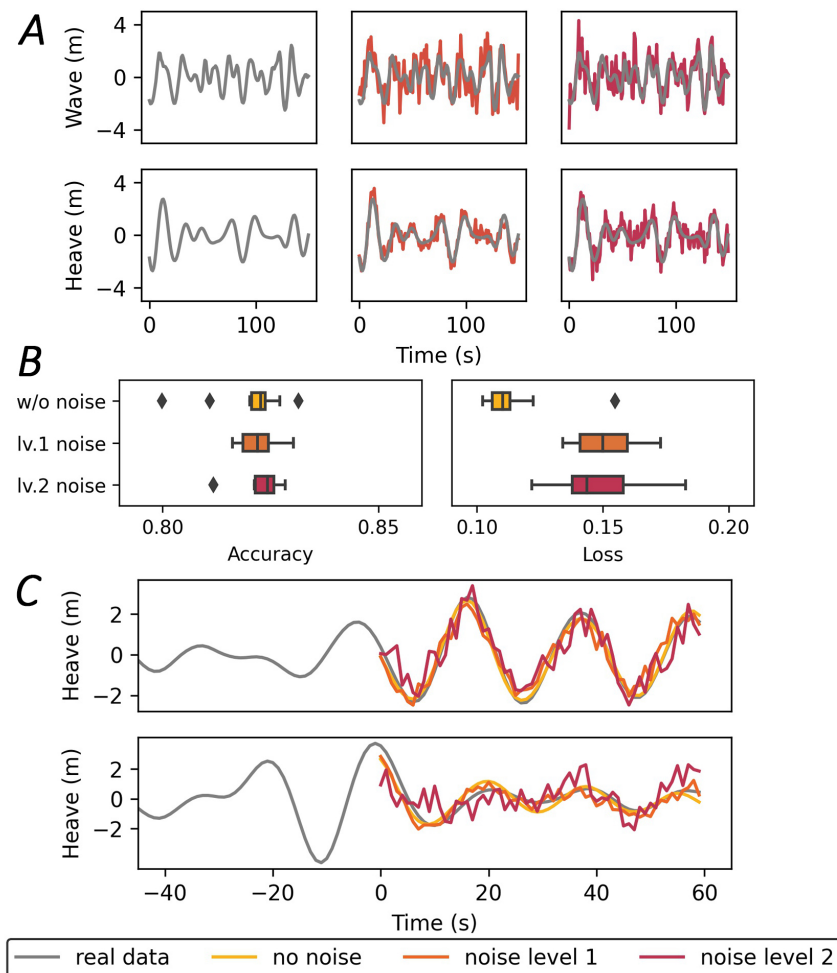


Figure 6. Training on different noise levels. (A) shows the data under different added noise levels; (B) shows the box plots of training results; (C) shows the motion prediction under different noise situations.

This is intuitive because the noise signal did not disturb the training data, which is typically unrelated to the original data. Therefore, using these training data in the model naturally yields a high accuracy. However, as the figure shows, the noisy data demonstrated better prediction performance at certain intervals. In other words, the noisy signals provide some degree of robustness to the model, thus allowing it to adapt to the uncertainty caused by noise or measurement errors, ultimately resulting in more accurate prediction of the motion time history.

3.4. Training on Transfer Learning Datasets

Pretraining is a typical training technique in deep learning and is used widely in model training. Pretraining models are important for NN models with numerous parameters (e.g., transformers) as they can reduce the time cost spent on training and play a role in determining the final performance of the model.

The main idea of pretraining a model is to first train it on an existing dataset and then fine-tune it on an actual application dataset such that the fine-tuned model can attain a

certain accuracy without excessive training. However, pretraining the model requires a significant amount of data support, and the data must be valid and reliable such that the model can adapt to deeper feature extraction; otherwise, the model may only be applied to a specific situation, i.e., the model's generalizability is inferior.

Therefore, data loads from diverse offshore platforms were included in the proposed dataset to ensure generalization. In particular, the dataset for this section comprises only data for the 100-year wave condition, which accounts for a significant portion of the dataset, as shown in Table 2. In the actual pretraining process, the prediction results similarly indicate this dataset's effectiveness in satisfying the pretraining task's requirements.

This subsection illustrates the effectiveness of this dataset in pretraining transfer learning in terms of domain adaptation and domain generalization. Transfer learning for domain adaptation and domain generalization typically relies on transfer learning algorithms, such as DANN (domain-adversarial neural network), to eliminate bias between different domains and achieve the final transfer learning effect. However, in this study, no additional transfer learning algorithms were applied, and the model was trained on the subsets and then fine-tuned to achieve the final results. Users can conduct further studies based on these datasets and use other transfer learning techniques.

3.4.1. Domain Adaptation

Domain adaptation refers to using data from the same domain for training and testing the prediction model. This implies that the model has already learned specific features related to the test data in advance, thus allowing it to recognize and interpret similar data during the testing phase.

The pretrained model initially uses a comprehensive subset of data that includes hundreds of samples from all 13 platforms. This broad dataset ensures that the model is exposed to a wide range of features and scenarios, thereby achieving solid foundational understanding. Subsequently, the model is fine-tuned using additional separate data from Platform 13, thus allowing it to adapt to and specialize in the specific characteristics of the platform. By contrast, the model without pretraining is trained and tested directly using only data from Platform 13. This approach tests the model's ability to learn and predict effectively without requiring prior exposure to a broader range of data, thus offering a comparison to assess the effect and value of the pretraining process.

Figure 7 illustrates the training results related to domain adaptation and generalization, emphasizing the domain adaptation subsets in Figure 7A. In the first row of the subfigure, the model's prediction accuracy is compared five times, both with and without pretraining. The results clearly show that the pretrained model consistently outperformed the non-pretrained version in terms of accuracy and exhibited a more stable loss pattern. The second row focuses on the model's predictions for a specific motion time-history clip. The comparison reveals that the predictions of the pretrained model were aligned more closely with the actual values. In the third row, a comparison of the best prediction results for the models with and without pretraining is shown, illustrating their training accuracy and loss over various epochs. As shown, the pretrained model began with a higher training accuracy, a lower training loss, and fewer epochs to achieve higher accuracy. In comparing the predicted curves with the actual motion curves shown in the final subfigure, both the pretrained and non-pretrained models performed similarly, in general, thus demonstrating the robustness of the pretraining.

Comparisons of various prediction results and processes revealed that the model with pretraining not only achieved higher accuracy but also required less time for training compared with the model without pretraining. This outcome was as expected because the pretraining phase included similar data from the target domain. However, a pertinent question arises: If pretraining solely involves data from other platforms, excluding any data from the current platform, will the model still maintain its high accuracy? Conversely, will the data from different platforms result in a "misleading" prediction trend for the current platform? These considerations delve into domain generalization, which will be discussed

in the following subsection. This investigation is crucial for understanding the broader applicability and limitations of pretraining in predictive modeling.

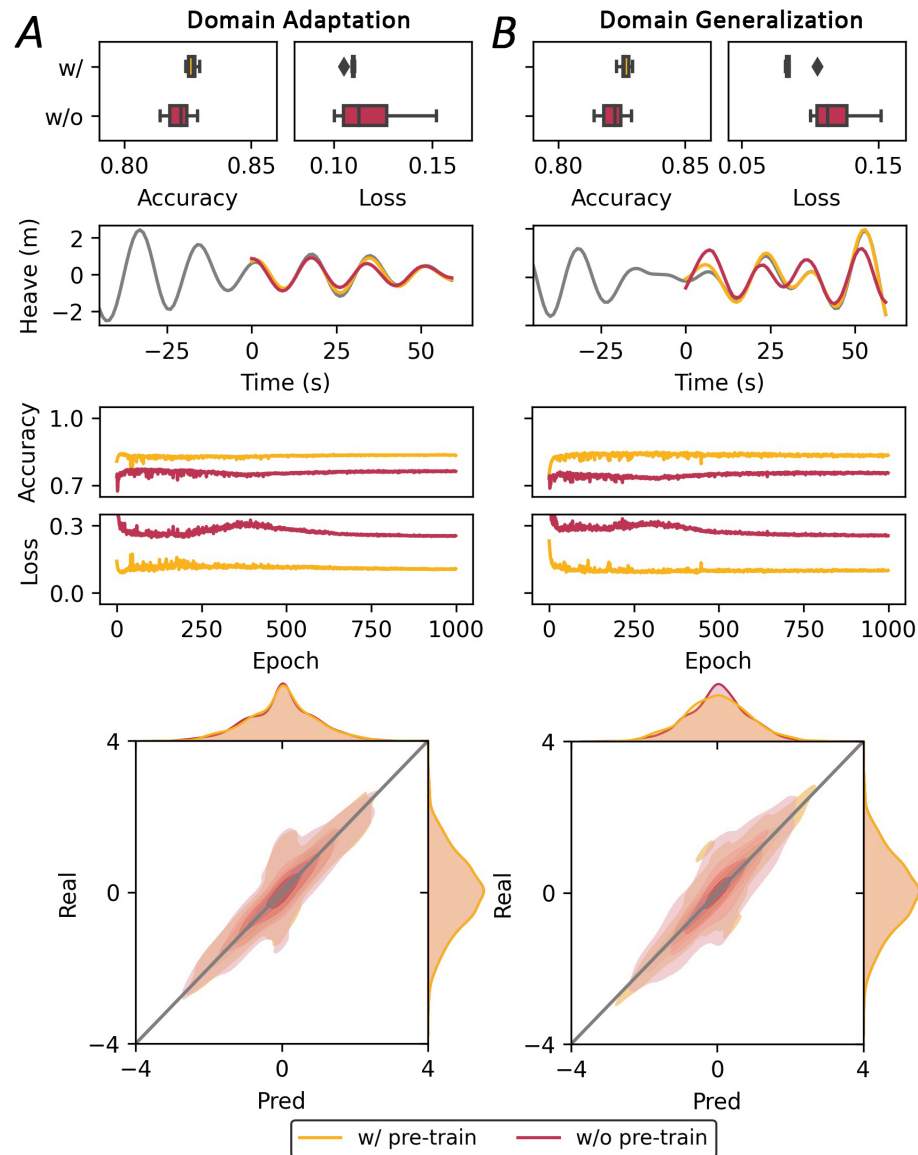


Figure 7. Training results of (A) domain adaptation and (B) domain generalization.

3.4.2. Domain Generalization

Domain generalization refers to a scenario in which the data utilized for pretraining originate exclusively from platforms other than the one currently targeted. This implies that the model is initially exposed to and learns features from the motions of different platforms, without any prior exposure to a specific platform for which it will be used. This approach tests the generality and universality of the dataset. If the data in the dataset are highly platform-specific and do not exhibit general applicability, then the model’s effectiveness can be limited, thus rendering it suitable only for the motion prediction of specific offshore platforms. Thus, domain generalization is an important criterion for evaluating the versatility and broad applicability of both the dataset and predictive model.

For the pretrained version of the model, the training dataset excludes data from Platform 13; instead, it comprises data from 12 other platforms. Subsequently, the model is fine-tuned and tested using additional data from Platform 13. The model without pretraining is consistently trained and tested using only data from Platform 13, similar to the

case of domain adaptation. Figure 7B shows the training results of domain generalization, with emphasis on the domain adaptation subsets in Figure 7A.

Similar to the result presented in the previous subsection, the model with pretraining performed better than that without pretraining; it shows a higher accuracy, lower losses, and a steadier training process. Furthermore, the model with pretraining learns the features of the general motion pattern on many platform data rather than on a specific platform; thus, it can extract the features of the current platform motion data more effectively. This proves the validity of the data in this dataset.

Based on the findings from Section 3.4.1, whereas the final prediction accuracy between the models with and without pretraining did not differ significantly, the pretrained models demonstrated higher learning efficiency throughout the training process. This efficiency is key in reducing the time and hardware costs of training larger models.

The training results further indicate that the dataset is well distributed and adaptable for use with multi-platform deep learning prediction models and for transfer learning algorithm investigations. Its diverse and comprehensive nature renders it an ideal standard benchmark for evaluating the predictive capabilities of various models. The dataset's adaptability and representativeness validate its utility for developing and testing models across different offshore platforms, reinforcing its value in marine motion prediction.

3.5. Results

In addition to utilizing the models for training on the dataset introduced herein, we extended the analysis to include models from previously cited references. We compared their prediction effectiveness using the same dataset. Each of these external models was trained on the specific sub-datasets shown in Figure 3.

To comprehensively evaluate their performances, several key metrics were calculated for each model:

1. Mean absolute error (MAE): This metric measures the average magnitude of the errors in a set of predictions without considering their direction. It can be calculated as follows:

$$MAE = \frac{1}{n} \sum |x_i - y_i| \quad i = 1, 2, \dots, n$$

Here, n denotes the length of x and y .

2. Mean squared error (MSE): The MSE assesses the average squared difference between the estimated and actual values, thus providing insight into the precision of the model.

$$MSE = \frac{1}{n} \sum (x_i - y_i)^2 \quad i = 1, 2, \dots, n$$

Here, n denotes the length of x and y .

3. Dynamic time warping accuracy (DTWAcc): This metric measures the similarity between two temporal sequences, which may vary in amplitude and phase. It can be calculated as follows:

$$DTWAcc = 1 - \sqrt{\frac{DTWDist(x, y)}{n}}$$

$DTWDist$ denotes the function to calculate the distance between x and y , which was first introduced in [44]; and n denotes the length of x and y .

4. Area Accuracy (AreaAcc): This metric evaluates the model's accuracy in predicting the overall shape and area under the curve of the motion trajectory. It can be calculated as follows:

$$AreaAcc = 1 - \left| 1 - \frac{Area(x)}{Area(y)} \right|$$

Here, $Area$ denotes the function used to calculate the area of x and y , such as the trapezoidal and Simpson rules.

Table 5 compares the performance of four models (LSTM, BiLSTM, Bi-ConvLSTM-CA, and ours) across various dataset subsets. Overall, our model demonstrates superior performance across all subsets. In both the Plat subset and Wave subset, our model stands out significantly, achieving the highest accuracy (88.4%, 98.2%). As for the Noise subset, the bi-directional LSTM can simultaneously process data in both forward and backward time sequences, making it effective at mitigating the impact of noise disturbances, and demonstrating superior performance with higher accuracy and lower loss. Although the Noise subset shows slightly higher error rates for our model, it still maintains competitive accuracy scores. This indicates that while noise impacts error, the overall performance remains within an acceptable range. In tests of adaptability and generalization (Adaptation subset and Generalization subset), our model displays strong generalization capabilities and consistent performance across different conditions, which highlights the model’s robustness and adaptability when handling complex and varied datasets.

Table 5. Comparison among different models trained on our dataset. (1) Plat subset primarily uses data from Platform 13. (2) Wave subset primarily uses data under 100-year wave conditions. (3) Noise subset primarily uses noise addition data at level 1. (4) Tf subset is classified into pretraining and fine-tuning sets, and the results shown in the table are those obtained after fine-tuning. * The bold means the best value in each metrics

Dataset	Model	MAE ↓	MSE ↓	DTW Acc ↑	Area Acc ↑
Plat subset	LSTM	0.441	0.347	73.2	80.7
	BiLSTM	0.455	0.363	73.1	79.2
	Bi-ConvLSTM-CA	0.432	0.334	74.3	81.5
	Ours	0.244 *	0.104	81.8	88.4
Wave subset	LSTM	0.362	0.231	76.1	82.0
	BiLSTM	0.344	0.213	77.1	83.3
	Bi-ConvLSTM-CA	0.358	0.230	76.6	82.3
	Ours	0.027	0.001	96.8	98.2
Noise subset	LSTM	0.472	0.378	72.2	78.7
	BiLSTM	0.463	0.358	71.9	79.7
	Bi-ConvLSTM-CA	0.472	0.379	72.4	78.9
	Ours	0.487	0.386	69.9	76.4
Tf subset Adaptation	LSTM	0.386	0.266	75.5	82.5
	BiLSTM	0.368	0.249	76.2	83.4
	Bi-ConvLSTM-CA	0.402	0.289	75.3	82.0
	Ours	0.248	0.110	82.7	86.2
Generalization	LSTM	0.429	0.329	73.8	80.8
	BiLSTM	0.385	0.268	75.7	82.5
	Bi-ConvLSTM-CA	0.432	0.336	74.7	81.6
	Ours	0.217	0.079	83.7	89.5

The calculation of these metrics is key in this study as it facilitates a comprehensive comparison of the predictive capabilities of the various models. This comparative analysis is crucial for validating the effectiveness and broad applicability of the dataset across different predictive modeling scenarios. As illustrated in Table 5, the results not only enable a clear comparison of performance across different models but also highlight the effectiveness of the model introduced herein.

4. Conclusions

This study introduces a novel dataset with a substantial amount of reliable test data and a cutting-edge machine learning model that achieves high accuracy across various tasks. The dataset establishes a new benchmark for motion prediction analysis, allowing the performance of different machine learning models to be easily assessed across four

dimensions. Furthermore, the Conv-Att-LSTM model integrates a self-attention mechanism and convolutional operations, significantly improving prediction accuracy.

- (1) The dataset proposed herein contributed significantly to marine motion prediction. It encompassed extensive model test data from the SKLOE and included 1-year to 1000-year wave environmental conditions. The dataset is a reliable and effective training resource classified into different usage scenarios. A demonstration version of this dataset is available to all researchers interested in ship and ocean platform motion prediction, and the full database can be accessed upon request from the authors.
- (2) In addition to the dataset, this study introduced a novel prediction model known as the Conv-Att-LSTM model, which integrates LSTM and self-attention mechanisms to achieve better predictions and lower training costs. The model was trained on the proposed dataset and benchmarked against several other models, demonstrating its superior accuracy and utility for motion prediction under different application scenarios.

This study demonstrates the immediate effectiveness of these methods and facilitates future related investigations, but there are still some drawbacks to be addressed, such as more efficient prediction models and comprehensive datasets. Therefore, future efforts will focus on broadening the scope of the dataset and enhancing its applicability and utility. This expanded dataset is a foundational tool for developing more sophisticated and effective machine learning models. The results obtained in this study suggest potential breakthroughs in marine technology and predictive analysis. Continued research and development in this area, such as state-of-the-art models with higher accuracy for motion prediction and more comprehensive datasets involving a wide range of different offshore platforms and ships, can significantly advance marine navigation, safety, and operational efficiency.

Author Contributions: Methodology, X.G. and W.P.; Resources, X.L.; Data curation, W.P.; Writing—original draft, W.P.; Writing—review & editing, X.G.; Supervision, X.L.; Funding acquisition, X.L. All authors have read and agreed to the published version of the manuscript.

Funding: This work is supported by the National Natural Science Foundation of China (Grant, No. 42206228) and the Hainan Province Natural Science Foundation (521QN276).

Data Availability Statement: Data are contained within the article.

Conflicts of Interest: The authors declare no conflict of interest.

References

1. Shi, Q.; Hu, C.; Li, X.; Guo, X.; Yang, J. Finite-time adaptive anti-disturbance constrained control design for dynamic positioning of marine vessels with simulation and model-scale tests. *Ocean Eng.* **2023**, *277*, 114117. [[CrossRef](#)]
2. Huang, L.; Duan, W.; Han, Y.; Chen, Y. A review of short-term prediction techniques for ship motions in seaway. *J. Ship Mech.* **2014**, *18*, 1534–1542.
3. Wei, H.; Xiao, L.; Tian, X.; Zhang, B.; Lu, W. A Hybrid Vision-based Method of Encountered Wave Field Measurement for Navigating Surface Vehicles. *IEEE Sens. J.* **2023**, *23*, 26850–26862. [[CrossRef](#)]
4. Kaplan, P. A Preliminary Study of Prediction Techniques for Aircraft Carrier Motions at Sea. *J. Hydronaut.* **1965**, *3*, 121–131.
5. Triantafyllou, M.; Athans, M. Real time estimation of the heaving and pitching motions of a ship, using a Kalman filter. In Proceedings of the OCEANS 81, Boston, MA, USA, 16–18 September 1981; pp. 1090–1095. [[CrossRef](#)]
6. Triantafyllou, M.; Bodson, M.; Athans, M. Real time estimation of ship motions using Kalman filtering techniques. *IEEE J. Ocean. Eng.* **1983**, *8*, 9–20. [[CrossRef](#)]
7. Yumori, I. Real time prediction of ship response to ocean waves using time series analysis. In Proceedings of the OCEANS 81, Boston, MA, USA, 16–18 September 1981; pp. 1082–1089. [[CrossRef](#)]
8. Duan, W.; Huang, L.; Han, Y.; Zhang, Y.; Huang, S. A hybrid AR-EMD-SVR model for the short-term prediction of nonlinear and non-stationary ship motion. *J. Zhejiang Univ.-SCIENCE A* **2015**, *16*, 562–576. [[CrossRef](#)]
9. Duan, W.; Huang, L.; Han, Y.; tai Huang, D. A hybrid EMD-AR model for nonlinear and non-stationary wave forecasting. *J. Zhejiang Univ.-SCIENCE A* **2016**, *17*, 115–129. [[CrossRef](#)]
10. Duan, W.; Han, Y.; Huang, L.; Zhao, B.B.; Wang, M.H. A hybrid EMD-SVR model for the short-term prediction of significant wave height. *Ocean Eng.* **2016**, *124*, 54–73. [[CrossRef](#)]

11. Jiang, H.; Duan, S.; Huang, L.; Han, Y.; Yang, H.; Ma, Q. Scale effects in AR model real-time ship motion prediction. *Ocean Eng.* **2020**, *203*, 107202. [[CrossRef](#)]
12. Lainiotis, D.; Plataniotis, K.; Penon, D.; Charalampous, C.J. Neural network application to ship position estimation. In Proceedings of the OCEANS '93, Victoria, BC, Canada, 18–21 October 1993; Volume 1, pp. I384–I389.
13. Khan, A.; Bil, C.; Marion, K.E. Ship motion prediction for launch and recovery of air vehicles. In Proceedings of the OCEANS 2005 MTS/IEEE, Washington, DC, USA, 17–23 September 2005; pp. 2795–2801.
14. Khan, A.; Marion, K.E.; Bil, C. The Prediction of Ship Motions and Attitudes using Artificial Neural Networks. In Proceedings of the 19th National Conference of the Australian Society for Operations Research, Melbourne, Australia, 3–5 December 2007.
15. Yin, J.; Perakis, A.N.; Wang, N. A real-time ship roll motion prediction using wavelet transform and variable RBF network. *Ocean Eng.* **2018**, *160*, 10–19. [[CrossRef](#)]
16. Hochreiter, S.; Schmidhuber, J. Long short-term memory. *Neural Comput.* **1997**, *9*, 1735–1780. [[CrossRef](#)]
17. Liu, Y.; Zheng, Q.; Duan, W.; Huang, L. Improving deterministic pitch motions estimation using bivariate sequential wave input. *IOP Conf. Ser. Mater. Sci. Eng.* **2019**, *688*, 033017. [[CrossRef](#)]
18. Liu, Y.; Duan, W.; Huang, L.; Duan, S.; Ma, X. The input vector space optimization for LSTM deep learning model in real-time prediction of ship motions. *Ocean Eng.* **2020**, *213*, 107681. [[CrossRef](#)]
19. Guo, X.; Zhang, X.; Tian, X.; Li, X.; Lu, W. Predicting heave and surge motions of a semi-submersible with neural networks. *Appl. Ocean Res.* **2021**, *112*, 102708. [[CrossRef](#)]
20. Guo, X.; Zhang, X.; Tian, X.; Lu, W.; Li, X. Probabilistic prediction of the heave motions of a semi-submersible by a deep learning problem model. *arXiv* **2021**, arXiv:2111.00873.
21. Sun, Q.; Tang, Z.; Gao, J.; Zhang, G. Short-term ship motion attitude prediction based on LSTM and GPR. *Appl. Ocean Res.* **2021**, *118*, 102927. [[CrossRef](#)]
22. Zhang, T.; Zheng, X.; Liu, M. Multiscale attention-based LSTM for ship motion prediction. *Ocean Eng.* **2021**, *230*, 109066. [[CrossRef](#)]
23. Li, H.; Xiao, L.; Wei, H.; Liu, M. Research on on-line prediction of floating offshore platform motions based on LSTM network. *J. Ship Mech.* **2021**, *25*, 576–585.
24. Wei, Y.; Chen, Z.; Zhao, C.; Tu, Y.; Chen, X.; Yang, R. A BiLSTM hybrid model for ship roll multi-step forecasting based on decomposition and hyperparameter optimization. *Ocean Eng.* **2021**, *242*, 110138. [[CrossRef](#)]
25. Fu, H.; Gu, Z.; Wang, Y. Ship Pitch Prediction Based on Bi-ConvLSTM-CA Model. *J. Mar. Sci. Eng.* **2022**, *10*, 840. [[CrossRef](#)]
26. Taskar, B.; Chua, K.H.; Akamatsu, T.; Kakuta, R.; Yeow, S.W.; Niki, R.; Nishizawa, K.; Magee, A. Real-Time Ship Motion Prediction Using Artificial Neural Network. In Proceedings of the ASME 2022 41st International Conference on Ocean, Offshore and Arctic Engineering, Hamburg, Germany, 5–10 June 2022; p. V05BT12A01.
27. Xun, S.; Zhu, P.; Yang, B.; Xiong, J. Multi-Direction Prediction Based on SALSTM Model for Ship Motion. In Proceedings of the 5th International Conference on Information Science, Electrical, and Automation Engineering (ISEAE 2023), Wuhan, China, 10 August 2023; pp. 127483F.1–127483F.10.
28. Chen, Z.; Liu, X.; Ji, X.; Gui, H. Real-Time Prediction of Multi-Degree-of-Freedom Ship Motion and Resting Periods Using LSTM Networks. *J. Mar. Sci. Eng.* **2024**, *12*, 1591. [[CrossRef](#)]
29. Yildiz, B. Prediction of residual resistance of a trimaran vessel by using an artificial neural network. *Brodogr. Int. J. Nav. Archit. Ocean Eng. Res. Dev.* **2022**, *73*, 127–140. [[CrossRef](#)]
30. Mentes, A.; Yetkin, M. An application of soft computing techniques to predict dynamic behaviour of mooring systems. *Brodogr. Int. J. Nav. Archit. Ocean Eng. Res. Dev.* **2022**, *73*, 121–137. [[CrossRef](#)]
31. Ozsari, I. Predicting main engine power and emissions for container, cargo, and tanker ships with artificial neural network analysis. *Brodogr. Int. J. Nav. Archit. Ocean Eng. Res. Dev.* **2023**, *74*, 77–94. [[CrossRef](#)]
32. Ma, Y.; Xu, Y.; Li, B.; Xi, Y. Research on coupling prediction of motion response of floating offshore platform. *Ship Sci. Technol.* **2017**, *39*, 94–99.
33. Xu, G.; Shi, F.; Liu, X.; Zhu, K. Numerical comparison of motion response prediction methods of Truss Spar platform in waves and currents. *Ocean Eng.* **2019**, *37*, 102–110.142.
34. Zhang, F.; Hou, J.; Ning, D.; Zhang, W.; Wang D.; Gong, Y. Performance analysis of the passive heave compensator for hydraulic shipwreck lifting systems in twin-barge salvaging. *Ocean Eng.* **2023**, *280*, 114469. [[CrossRef](#)]
35. Lee, J.; Lee, J.; Kim, Y.; Ahn, Y. Prediction of wave-induced ship motions based on integrated neural network system and spatiotemporal wave-field data. *Physics Fluids* **2023**, *35*, 097127. [[CrossRef](#)]
36. Zhang, F.; Ning, D.; Hou, J.; Du, H.; Tian, H.; Zhang, K.; Gong, Y. Semi-Active Heave Compensation for a 600-Meter Hydraulic Salvaging Claw System with Ship Motion Prediction via LSTM Neural Networks *J. Mar. Sci. Eng.* **2023**, *11*, 998. [[CrossRef](#)]
37. Deng, J.; Dong, W.; Socher, R.; Li, L.J.; Li, K.; Fei-Fei, L. Imagenet: A large-scale hierarchical image database. In Proceedings of the 2009 IEEE Conference on Computer Vision and Pattern Recognition, Miami, FL, USA, 20–25 June 2009; pp. 248–255.
38. Carreira, J.; Zisserman, A. Quo vadis, action recognition? A new model and the kinetics dataset. In Proceedings of the IEEE Conference on Computer Vision and Pattern Recognition, Honolulu, HI, USA, 21–26 July 2017; pp. 6299–6308.
39. Soomro, K.; Zamir, A.R.; Shah, M. A dataset of 101 human action classes from videos in the wild. *Cent. Res. Comput. Vis.* **2012**, *2*, 1–7.

40. Kuehne, H.; Jhuang, H.; Garrote, E.; Poggio, T.; Serre, T. HMDB: A large video database for human motion recognition. In Proceedings of the 2011 International Conference on Computer Vision, Barcelona, Spain, 6–13 November 2011; pp. 2556–2563.
41. LeCun, Y.; Bottou, L.; Bengio, Y.; Haffner, P. Gradient-based learning applied to document recognition. *Proc. IEEE* **1998**, *86*, 2278–2324. [[CrossRef](#)]
42. Liu, Z.; Luo, P.; Wang, X.; Tang, X. Deep learning face attributes in the wild. In Proceedings of the IEEE International Conference on Computer Vision, Santiago, Chile, 7–13 December 2015; pp. 3730–3738.
43. Zheng, W.; Lu, B. Investigating critical frequency bands and channels for EEG-based emotion recognition with deep neural networks. *IEEE Trans. Auton. Ment. Dev.* **2015**, *7*, 162–175. [[CrossRef](#)]
44. Thanawin R.; Bilson C.; Abdullah M.; Gustavo B.; Brandon W.; Qiang Z.; Jesin Z.; Eamonn K. Searching and mining trillions of time series subsequences under dynamic time warping. In Proceedings of the 18th ACM SIGKDD International Conference on Knowledge Discovery and Data Mining, Beijing, China, 12–16 August 2012; pp. 262–270.

Disclaimer/Publisher’s Note: The statements, opinions and data contained in all publications are solely those of the individual author(s) and contributor(s) and not of MDPI and/or the editor(s). MDPI and/or the editor(s) disclaim responsibility for any injury to people or property resulting from any ideas, methods, instructions or products referred to in the content.